American Mineralogist, Volume 76, pages 1002–1017, 1991

Highly aluminous hornblende from low-pressure metacarbonates and a preliminary thermodynamic model for the Al content of calcic amphibole

Albert Léger, John M. Ferry

Department of Earth and Planetary Sciences, The Johns Hopkins University, Baltimore, Maryland 21218, U.S.A.

Abstract

Calcic amphiboles in carbonate rocks at the same metamorphic grade from the Waits River Formation, northern Vermont, contain 2.29–19.06 wt% Al_2O_3 (0.38–3.30 Al atoms per formula unit, pfu). These Al-rich amphibole samples are among the most aluminous examples of hornblende ever analyzed. The amphibole-bearing metacarbonates are interbedded with andalusite-bearing pelitic schists and therefore crystallized at $P < 3800$ bars. These results demonstrate that factors in addition to pressure must control Al content in hornblende. We have identified temperature, mineral assemblage, mineral composition, and rock chemistry [especially Fe/(Fe + Mg)] as other important factors.

To explore semiquantitatively the dependence of the Al content of calcic amphibole on *P, T,* and coexisting mineral assemblage, a simple thermodynamic model was developed for mineral equilibria involving tremolite-tschermakite ($[Ca_2Mg_5Si_8O_{22}(OH)_2]$-$[Ca_2Mg_3Al_4Si_6O_{22}(OH)_2]$) amphibole solutions. The model uses the thermodynamic data base of Berman (1988), with the addition of new values for standard-state enthalpy and entropy for pure end-member tschermakite derived from experimental and field data on the Al content in tremolite coexisting with diopside, anorthite, and quartz. Calculated phase equilibria lead to three conclusions: (1) At a specified *P* and *T,* the Al content of calcic amphibole is strongly dependent on the coexisting mineral assemblage. (2) No universal relationship exists between the Al content of amphibole and *P.* (3) The Al content of amphibole may change dramatically with changes in *P* and *T.* Maximum Al contents calculated by the model are ~1.2 Al atoms pfu. These values are far short of the 3.30 Al atoms pfu measured in some amphibole samples from Vermont. The principal shortcoming of the model is its failure to consider both total Fe in amphibole and the partitioning of Fe and Mg among the M1, M2, and M3 crystallographic sites.

Introduction

The chemical complexity of hornblende has long been of interest to petrologists because of its potential as a record of intensive variables during amphibole crystallization. Recently, studies have focused on the Al content of hornblende as a practical geobarometer. Experimental and empirical studies, for example, show that a positive correlation exists between total pressure and the Al content of hornblende in certain assemblages of minerals and silicate melt (Hammarstrom and Zen, 1986; Hollister et al., 1987; Johnson and Rutherford, 1989a, 1989b). The Al content in hornblende is thus regarded as a useful geobarometer for appropriate plutonic and volcanic rocks. Highly aluminous amphibole is likewise often regarded as an indicator of high-pressure metamorphic rocks because it is found coexisting with jadeite, kyanite, or glaucophane (Leake, 1965a, 1965b; Kostyuk and Sobolev, 1969; Raase, 1974; Selverstone et al., 1984). Moreover, some experimental studies of mineral assemblages relevant to metamorphic rocks have shown that a positive correlation exists between the Al content of hornblende and pressure (cf. Spear, 1981; Pluysnina, 1982; Cao et al., 1986; Jenkins, 1988, 1989).

It came as a surprise, therefore, that during a regional study of the progressive metamorphism of marls from the Waits River Formation, northeast Vermont, we found some hornblende samples with unusually high Al content. The most Al-rich amphibole samples in this study contain over 19 wt% Al_2O_3 (3.30 Al atoms pfu). These are among the most aluminous hornblende samples ever reported (cf. Leake, 1965a, 1965b, 1971; Doolan et al., 1978; Selverstone et al., 1984; Sawaki, 1989). Even though these hornblende samples have high Al content, they are neither from very aluminous rocks (the host marls have <15 wt% Al_2O_3) nor from rocks metamorphosed at elevated pressure (the marls are interbedded with andalusite-bearing schists and crystallized at $P < 3800$ bars).

Our second major observation is that the Al content of hornblende varies greatly (from ~0.4 to 3.3 Al atoms pfu), even in marls from Vermont at the same metamorphic grade, depending on the coexisting mineral assem-

0003–004X/91/0506–1002$02.00

blage and mineral chemistry. Both observations indicate that some factor(s) other than pressure and temperature must exercise a first-order control on the Al content of amphibole. Our study identifies two such controls: (1) the assemblage of minerals coexisting with hornblende and (2) the composition of those minerals [particularly Fe/(Fe + Mg) and anorthite content of plagioclase]. We have developed a simple model for the Al content of tremolite-tschermakite solid solutions in the system K_2O-CaO-MgO-Al_2O_3-SiO_2-H_2O-CO_2. The model explains the dependence of the Al content of hornblende both on the coexisting mineral assemblage and the *P-T* conditions of crystallization. The model for this simple system, however, does not predict the high-Al hornblende observed in some rocks from Vermont. Further research must be completed before an adequate quantitative understanding of the Al content of calcic amphibole can be attained.

Geological setting of high-Al hornblende from Vermont

Hornblende-bearing metamorphosed marls were collected from the Siluro-Devonian Waits River Formation in northeastern Vermont (Fig. 1), which has been mapped by numerous geologists (Doll, 1951; Dennis, 1956; Hall, 1959; Cady, 1960; Konig and Dennis, 1964; Woodland, 1965). The formation consists of interbedded limestone (2–15 cm thick), argillaceous metacarbonates, and minor pelitic schists. The Waits River Formation, together with the adjacent and more pelitic Gile Mountain Formation, are part of the Connecticut Valley–Gaspe synclinorium. The structure and metamorphism now observed in the area developed primarily during the Devonian Acadian Orogeny (ca. 370–400 Ma). Two major folds, the Brownington syncline (Doll, 1951) on the western side of the synclinorium and the Strafford-Willoughby arch (Eric and Dennis, 1958) on the eastern side of the synclinorium control the regional attitude of beds. Beds strike northeast except where locally deflected around igneous intrusions.

The metasedimentary rocks were intruded by numerous late- to posttectonic granitic plutons of the New Hampshire Plutonic Series (Doll et al., 1961). From the distribution of isograds and metamorphic zones (Fig. 1), it is clear that the plutons were local heat sources for the highest grades of metamorphism attained in the area. With respect to pelitic schists, metamorphic grade ranges from chlorite zone to the sillimanite zone near the plutons. Garnet and amphibole porphyroblasts crosscut the main schistosity, indicating that the peak of medium- and high-grade metamorphism occurred after the last period of deformation. Four metamorphic zones were also mapped based on minerals in the metamorphosed marls (Fig. 1). The biotite isograd separates the ankerite zone at lower grade from the biotite zone at higher grade. The amphibole isograd separates the biotite and amphibole zones, and the diopside isograd separates the amphibole and diopside zones. Amphibole described in this study is from rocks of the amphibole and diopside zones.

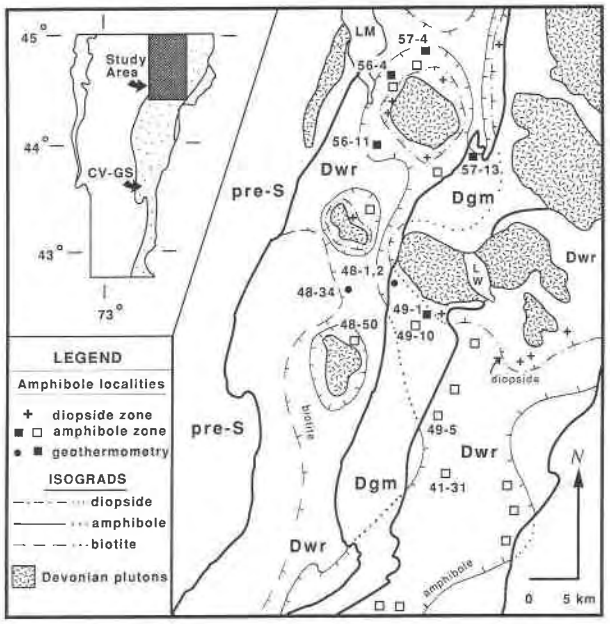

Fig. 1. Geologic sketch map of the area studied. Thick solid lines = stratigraphic boundary between Devonian Gile Mountain (Dgm) and Waits River (Dwr) Formations. Isograds are based on mineral assemblages in metacarbonate rocks and have hachures on their high-grade sides. Filled squares = amphibole localities with geothermometry; empty squares = other amphibole localities; filled circles: other geothermometry localities. LM = Lake Memphremagog; LW = Lake Willoughby; pre-S = pre-Silurian rocks; CV-GS = Connecticut Valley–Gaspe Synclinorium. Geologic map based on that of Doll et al. (1961).

Methods of investigation

Thirty-one samples of metamorphosed impure carbonate rock containing amphiboles were collected from 27 field localities (Fig. 1). Mineral assemblages were identified by petrographic observation of thin sections. Mineral compositions in all samples were determined by electron microprobe analysis using the JEOL JXA-8600 Superprobe at the Department of Earth and Planetary Sciences, The Johns Hopkins University, and natural mineral standards. Data for both silicates and carbonates were reduced with a ZAF correction scheme. Chemical analysis of 23 rock samples for major elements were performed by X-ray fluorescence: 13 at X-Ray Assay Laboratories, Ltd., Don Mills, Ontario, and ten at the Geochemical Laboratories, Department of Geological Sciences, McGill University, Montreal, Quebec.

Mineral content and chemistry and petrologic features of rocks with high-Al hornblende

Mineral assemblages observed in six representative specimens from the amphibole zone are listed in Table 1. These specimens were chosen to show the wide range in amphibole compositions (especially in Al_2O_3 content) even in marls metamorphosed at the same grade.

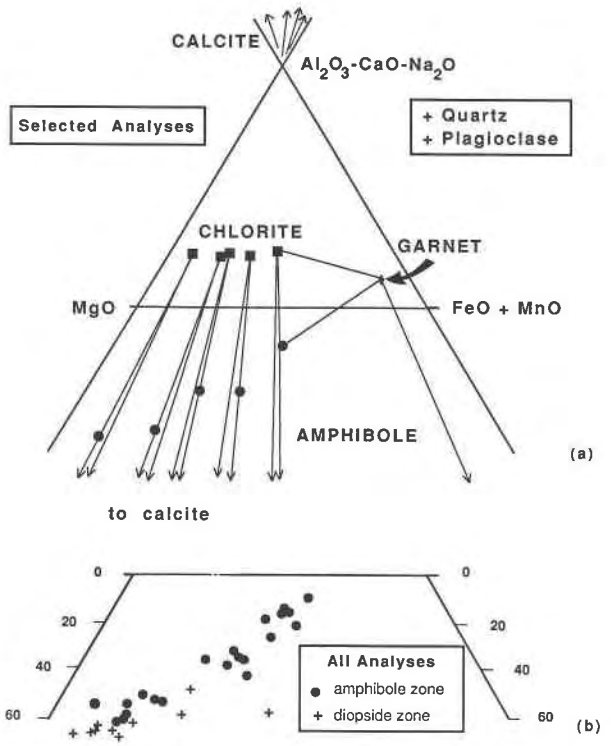

Fig. 2. (**a**) Chemographic relationships among minerals in five representative samples from the amphibole zone of Figure 1. Diagram refers to constant P and T and assemblages with plagioclase and quartz. Note the greater dependence of Al_2O_3 content in amphibole on (Fe + Mn)/(Fe + Mg + Mn) than in chlorite. (**b**) Same plot as in **a**; note positive correlation between (FeO + MnO) and Al_2O_3 in all amphibole samples analyzed from metacarbonates of the Waits River Formation, northern Vermont.

Mineral assemblages and mineral chemistry

Metamorphosed carbonate rocks from the amphibole zone in Figure 1 all contain calcite, quartz, plagioclase, amphibole, and biotite, along with combinations of titanite, sulfides, chlorite, clinozoisite, potassium feldspar, garnet, muscovite, ankerite, and ilmenite. Compositions of amphibole, biotite, chlorite, calcite, clinozoisite, garnet, and plagioclase for the six specimens listed in Table 1 are compiled in Table 2. Mineral compositions in Table 2 are typically an average of five to ten spot analyses of three to five grains. Except where otherwise stated, analyses represent rim compositions. The value of "oxide sum" refers to the conventional sum of metal oxide weight percentages with all Fe as FeO. No analyses of quartz, titanite, or sulfides were obtained. Minerals from the amphibole zone are described below.

Amphibole. Calcic amphiboles occur in all 23 specimens studied. They vary widely in composition from tremolite to ferro-tschermakite in the nomenclature of Leake (1978). Amphibole samples have 0.38–3.31 Al atoms and 7.81–6.18 Si atoms pfu and Fe/(Fe + Mg) = 0.15–0.62. The compositions of amphibole samples and coexisting chlorite, calcite, and garnet are plotted on Figure 2a for selected samples of metamorphosed marls from the amphibole zone of the Waits River Formation. The diagram approximates mineral compositions by the model system Na_2O-CaO-MgO-FeO-MnO-Al_2O_3-SiO_2-H_2O-CO_2, following the scheme of Robinson and Jaffe (1969). The compositions of amphibole samples alone in all samples analyzed from the amphibole and diopside zones are plotted in Figure 2b.

Two observations can be made from Figure 2: (1) A wide range of amphibole compositions crystallized at the same metamorphic grade. Amphibole from the diopside zone crystallized at higher temperature than that from the amphibole zone but are plotted on the same diagram for comparison. (2) A distinct, positive correlation exists between the Al_2O_3 content and (Fe + Mn)/(Fe + Mn + Mg) in amphibole. There is also a very weak positive correlation between the Al content and (Fe + Mn)/(Fe + Mn + Mg) of coexisting chlorite and biotite (see Table 2), but the correlation for chlorite is barely perceptible at the scale of Figure 2.

Low-Al amphibole samples generally are smaller in size than Al-rich counterparts and coexist with muscovite and

Table 1. Mineral abundances* in representative specimens from the amphibole zone, Waits River Formation, northern Vermont

	Sample number					
	49-10A	41-31	49-5	48-50	56-4C	56-11
Amphibole	0.38	0.32	0.82	0.17**	0.70	0.26
Calcite	18.37	14.77	11.09	5.22	7.85	6.70
Quartz	6.22	12.04	8.20	8.73	14.90	10.86
Biotite	0.34	0.12	0.35	1.56	0.08	0.11
Chlorite	—	0.07**	0.09**	0.01	0.15	0.42**
Plagioclase	0.25	0.55	1.02	3.14	0.91	3.04
Garnet	—	—	—	—	0.18**	0.14**
Clinozoisite	—	—	—	—	0.03**	0.004**
Ankerite	—	—	—	—	tr**	—
Ilmenite	—	—	—	0.10	0.09	0.20
Pyrrhotite	tr**	0.26**	tr**	0.37**	0.88**	tr**
Titanite	0.002	0.04	0.04	—	—	—

Note: The abbreviation tr indicates <0.05 vol%.
* Abundances are in moles/liter of metamorphic rock, calculated following the method of Ferry (1989).
** Modal abundance is determined directly by counting 2000 points in thin section.

TABLE 2. Representative mineral compositions

	Amphibole^ Sample number															
	49-10A		41-31		49-5		48-50		56-4C (core)		56-4C (edge)		56-11 (core)		56-11 (edge)	
K_2O	0.08		0.02		0.16		0.21		0.08		0.03		0.11		0.11	
Na_2O	0.49		0.57		0.88		1.19		1.25		1.16		1.62		1.55	
CaO	12.60		12.62		11.99		11.66		11.50		11.37		11.04		11.21	
MnO	0.00		0.15		0.64		0.25		0.26		0.28		0.21		0.21	
MgO	18.59		17.49		12.26		9.56		8.14		8.93		6.06		6.55	
FeO	7.21		8.20		13.42		14.47		15.36		15.32		17.78		17.03	
TiO_2	0.32		0.48		0.47		0.48		0.33		0.43		0.42		0.29	
Al_2O_3	4.78		4.91		10.22		15.92		18.19		16.09		19.06		18.99	
SiO_2	53.26		53.30		47.89		43.78		42.95		44.09		41.56		41.80	
Total	97.33		97.74		97.95		97.52		98.06		97.70		97.86		97.74	
	13CNK	Fe(+2)	13CNK	Fe(+2)	13CNK	Fe(+2)	13CNK	Fe(+2)	13CNK	Fe(+2)	13CNK	Fe(+2)	13CNK	Fe(+2)	13CNK	Fe(+2)
K	0.014	0.014	0.004	0.004	0.030	0.030	0.039	0.039	0.015	0.015	0.005	0.005	0.021	0.021	0.021	0.021
Na	0.015	0.121	0.056	0.105	0.094	0.228	0.150	0.291	0.136	0.289	0.092	0.265	0.201	0.340	0.204	0.335
Na	0.112	0.012	0.100	0.051	0.151	0.020	0.185	0.047	0.216	0.067	0.235	0.066	0.261	0.126	0.237	0.110
Ca	1.888	1.901	1.900	1.906	1.849	1.865	1.815	1.832	1.784	1.802	1.765	1.785	1.739	1.755	1.763	1.778
Mn		0.000		0.018		0.080		0.031		0.033		0.035		0.026		0.026
Fe^{2+}		0.087		0.025		0.035		0.090		0.098		0.114		0.093		0.086
Fe^{2+}	0.538	0.763	0.815	0.942	1.207	1.594	1.318	1.685	1.398	1.780	1.330	1.763	1.768	2.113	1.699	2.022
Mg	3.879	3.905	3.664	3.675	2.631	2.654	2.071	2.090	1.755	1.773	1.929	1.951	1.328	1.340	1.433	1.445
Mn	0.000		0.018		0.079		0.031		0.033		0.035		0.026		0.026	
Ti	0.034	0.034	0.051	0.051	0.050	0.051	0.053	0.053	0.036	0.036	0.046	0.047	0.047	0.047	0.032	0.032
Fe^{3+}	0.306		0.149		0.408		0.441		0.461		0.526		0.418		0.391	
$^{[6]}Al$	0.243	0.298	0.303	0.329	0.625	0.701	1.087	1.172	1.317	1.411	1.314	1.239	1.414	1.500	1.420	1.501
$^{[4]}Al$	0.546	0.496	0.511	0.487	1.109	1.048	1.639	1.580	1.786	1.723	1.613	1.540	1.889	1.833	1.865	1.812
Si	7.454	7.504	7.489	7.513	6.891	6.952	6.361	6.420	6.214	6.277	6.387	6.460	6.111	6.167	6.135	6.188
$Fe^{2+}/(Fe^{2+} + Mg)$	0.122	0.179	0.182	0.208	0.315	0.319	0.389	0.459	0.443	0.514	0.408	0.490	0.571	0.622	0.542	0.593
KNa_{-1}^{B}	0.014	0.014	0.004	0.004	0.030	0.030	0.039	0.039	0.015	0.015	0.005	0.005	0.021	0.021	0.021	0.021
$Fe^{2+}Mg_{-1}$	0.504	0.816	0.782	0.934	1.236	1.658	1.296	1.753	1.395	1.875	1.319	1.865	1.747	2.185	1.693	2.102
$Fe^{3+}Al_{-1}$	0.374	0.068	0.251	0.102	0.508	0.102	0.547	0.106	0.533	0.072	0.618	0.094	0.512	0.094	0.455	0.064
$MgCa_{-1}$	0.000	0.087	0.000	0.040	0.000	0.115	0.001	0.121	0.000	0.131	0.180	0.149	0.001	0.119	0.001	0.112
Plagioclase	0.112	0.012	0.100	0.054	0.151	0.020	0.184	0.047	0.216	0.067	0.055	0.066	0.260	0.126	0.236	0.110
Edenite	0.029	0.135	0.060	0.106	0.124	0.258	0.190	0.330	0.151	0.304	0.277	0.270	0.223	0.361	0.226	0.356
Tschermak	0.617	0.366	0.554	0.431	1.133	0.803	1.634	1.278	1.850	1.483	1.932	1.333	1.926	1.594	1.875	1.565
$TiFe^{2+}Fe^{3+}_{-2}$	0.034	0.034	0.051	0.051	0.050	0.051	0.053	0.053	0.036	0.036	0.046	0.047	0.047	0.047	0.032	0.032
$MnFe_{-1}$	0.000	0.000	0.018	0.018	0.079	0.080	0.031	0.031	0.033	0.033	0.035	0.035	0.026	0.026	0.026	0.026
Tremolite	1.000	1.000	1.000	1.000	1.000	1.000	1.000	1.000	1.000	1.000	1.000	1.000	1.000	1.000	1.000	1.000

TABLE 2—*Continued*

Biotites[C]

	Sample number					
	49-10A	41-31	49-5	48-50	56-4C	56-11
K	0.815	0.902	0.913	0.810	0.747	0.757
Na	0.016	0.020	0.009	0.023	0.035	0.013
Ca	0.013	0.020	0.004	0.009	0.004	0.006
Mn	0.002	0.004	0.020	0.004	0.003	0.010
Mg	1.744	1.755	1.403	1.454	1.124	1.002
Fe	0.742	0.670	0.966	0.921	1.209	1.252
Ti	0.087	0.071	0.098	0.083	0.079	0.084
$^{[6]}$Al	0.323	0.350	0.373	0.420	0.486	0.517
$^{[4]}$Al	1.162	1.177	1.217	1.207	1.255	1.224
Si	2.838	2.823	2.783	2.793	2.745	2.776
Oxide sum	95.57	96.44	95.63	95.74	96.09	95.98
Fe/(Fe + Mg)	0.300	0.276	0.408	0.388	0.518	0.555

Chlorites[D]

	Sample number				
	41-31	49-5	48-50	56-4C	56-11
Mn	0.008	0.051	0.011	0.011	0.009
Mg	3.531	2.885	2.894	2.333	2.042
Fe	1.059	1.622	1.611	2.127	2.441
Ti	0.007	0.003	0.012	0.004	0.012
Al	2.541	2.685	2.721	2.861	2.807
Si	2.784	2.700	2.681	2.610	2.630
Oxide sum	87.43	88.39	88.23	89.26	88.68
Fe/(Fe + Mg)	0.231	0.360	0.358	0.477	0.545

Calcite[E]

	Sample number					
	49-10A	41-31	49-5	48-50	56-4C	56-11
Ca	0.961	0.962	0.953	0.919	0.919	0.908
Fe	0.011	0.009	0.013	0.027	0.034	0.044
Mg	0.025	0.027	0.019	0.043	0.037	0.038
Mn	0.003	0.002	0.015	0.011	0.010	0.010
Oxide sum	56.26	56.11	55.95	56.24	56.03	56.06
Fe/(Fe + Mg)	0.306	0.237	0.277	0.333	0.420	0.478

Garnet[F]

	Sample number	
	56-4C	56-11
Ca	0.682	0.658
Mg	0.273	0.211
Mn	0.327	0.274
Fe^{2+}	1.698	1.820
Al	1.983	1.959
Fe^{3+}	0.033	0.075
Ti	0.005	0.003
Al	0.027	0.040
Si	2.973	2.960
Oxide sum	100.42	99.48

TABLE 2—*Continued*

	Clinozoisite[G]	
	Sample number	
	56-4C	56-11
Ca	1.896	1.899
Mg	0.012	0.011
Mn	0.027	0.017
Fe	0.363	0.397
Al	2.633	2.633
Ti	0.010	0.007
Si	3.026	3.007
Oxide sum	97.54	96.56

	Plagioclase					
	Sample number					
	49-10A	41-31	49-5	48-50	56-4C	56-11
X(An)	0.467	0.354	0.886	0.629	0.836	0.360
X(Ab)	0.530	0.646	0.114	0.370	0.164	0.638
X(Or)	0.003	0.000	0.000	0.001	0.000	0.002
Oxide sum	99.56	99.86	100.11	99.59	100.11	99.45
Range *X*(An)	0.28–0.48	0.26–0.39	0.84–0.91	0.53–0.67	0.78–0.89	0.24–0.44

[A] Amphibole renormalizations: 13 CNK = atoms per 13 cations (excluding Na, K, Ca); Fe(+2) = all Fe as Fe^{+2}.

[B] Exchange components (first nine rows) calculated following the method of Thompson (1982). Plagioclase = $CaAlNa_{-1}Si_{-1}$; edenite = $NaAlSi_{-1}$, Tschermak = $Al_2Mg_{-1}Si_{-1}$; Tremolite [$Ca_2Mg_5Si_8O_{22}(OH)_2$] is the additive component.

[C] Biotite: atoms per 11 O atoms (excluding H_2O).

[D] Chlorite: atoms per 14 O atoms (excluding H_2O).

[E] Calcite: cations per O atom (excluding CO_2).

[F] Garnet: cations per eight total cations.

[G] Clinozoisite: cations per 12.5 O atoms (excluding H_2O). All Fe in biotite, chlorite, and calcite considered Fe^{2+}; all Fe in clinozoisite considered Fe^{3+}; Fe^{3+}/Fe^{2+} ratios in amphibole and garnet adjusted to charge balance 23 and 12 O atoms, respectively.

TABLE 3. Representative whole-rock chemical analyses*

	Sample number					
	49-10A	41-31	49-5	48-50	56-4C	56-11
SiO_2	23.40	34.80	36.70	47.14	48.20	47.80
Al_2O_3	2.21	2.45	7.49	14.92	8.35	12.20
TiO_2	0.13	0.17	0.33	0.68	0.37	0.64
Fe_2O_3**	2.14	2.41	5.53	7.02	8.90	7.39
MgO	3.78	2.81	4.50	4.09	3.14	2.16
MnO	0.15	0.14	0.58	0.17	0.59	0.29
CaO	37.90	29.72	25.80	14.33	18.70	15.60
Na_2O	0.21	0.21	0.23	0.78	0.42	2.23
K_2O	0.49	0.18	0.57	2.16	0.10	0.15
P_2O_5	0.05	0.07	0.31	0.12	0.25	0.15
LOI†	29.60	27.06	18.20	8.85	11.50	11.60
Total	100.06	100.02	100.24	100.26	100.52	100.21

* Weight percent. Detection limit for major elements: 0.01%; for P_2O_5: 10 ppm.
** All Fe as Fe_2O_3.
† Loss on ignition.

potassium feldspar. Amphibole with high Al_2O_3 contents usually occurs as porphyroblasts and coexists with garnet and other minerals with high Fe/(Fe + Mg) (i.e., chlorite and biotite). In some specimens (e.g., 56-4C) amphibole is zoned with higher Al_2O_3 contents at the core than at the rim. In other specimens (e.g., 56-11), however, amphibole shows no significant zonation in Al_2O_3 (Table 2).

Amphibole from specimen 56-11, the sample having the highest Al_2O_3 content (19.06 wt% at the core), was examined with the transmission electron microscope (TEM) at the Johns Hopkins University by E. Smelik to test whether the high Al content was possibly the result of submicroscopic Al-rich inclusions that might not be detected at the scale of electron microprobe analysis. Results from TEM observations demonstrate that the amphibole samples analyzed are homogeneous, monomineralic phases and contain no submicroscopic inclusions of any kind.

Coexisting minerals. Plagioclase occurs in all samples and its composition varies greatly, both within and between specimens. Potassium feldspar occurs in four specimens from the amphibole zone. The range in measured potassium feldspar composition is small, K/(K + Na) = 0.94–0.99.

Biotite occurs in 17 specimens with Fe/(Fe + Mg) varying between 0.11 and 0.56 and $^{[6]}Al$ = 0.30–0.52 atoms pfu. Chlorite occurs in 11 specimens with Fe/(Fe + Mg) = 0.11–0.55 and Al_{tot} = 2.52–2.81 atoms pfu. Muscovite occurs in four specimens with K/(K + Na) = 0.98–0.99 and 3.17–3.25 Si atoms pfu.

Garnet coexists with the most aluminous amphiboles analyzed (samples 49-1A, 56-4C, and 56-11). The garnets are normally zoned and show near-perfect hexagonal outline in thin section with radiating inclusion trails. Schistosity is not deflected around the porphytoblasts, indicating that garnet grew during static metamorphism.

Clinozoisite was observed in five specimens; it is close to a $Ca_2(Al,Fe)_3Si_3O_{12}(OH)$ solid solution with Al/(Al + Fe) = 0.87–0.98.

All samples contain calcite that is close to pure $CaCO_3$ (0.91–0.99 Ca atoms pfu).

Whole-rock chemistry and the prograde amphibole-forming reaction

Major element chemical analyses were obtained for all amphibole-zone specimens from the Waits River Formation. Analyses for the six representative samples in Table 1 are listed in Table 3. The principal observation from results in Table 3 is that, compared to pelitic rocks, the Al-rich hornblende is not from Al-rich rocks. All whole-rock specimens analyzed have <15 wt% Al_2O_3. Prograde amphibole-forming reactions were derived using whole-rock chemical and mineral-chemical data in Tables 2 and 3, following the method outlined by Ferry (1989). The reactions typically are of the form ankerite + quartz + plagioclase + rutile + H_2O = amphibole + calcite + chlorite + titanite + CO_2.

Physical conditions during metamorphism

Metacarbonate rocks from the Waits River Formation in northeastern Vermont are interbedded with andalusite-bearing metapelites. The study area is close to, but on the low-pressure side of, the aluminum-silicate triple point isobar as mapped by Thompson and Norton (1968). Pressure therefore was <3.8 kbar (Holdaway, 1971). To a first approximation, the pressure during metamorphism was considered ~3500 ± 500 bars throughout the study area.

Peak metamorphic temperature in the amphibole zone was estimated using garnet-biotite, garnet-ilmenite, and calcite-dolomite geothermometry. Results for 18 rocks from nine field localities (see Fig. 1) containing appropriate mineral assemblages are listed in Appendix Table 1. The preferred estimate of the average temperature for the amphibole zone, calculated with the three different geothermometers, is 525 ± 30 °C.

PRELIMINARY THERMODYNAMIC MODEL FOR Al SUBSTITUTION IN CALCIC AMPHIBOLE

The unusually high Al content of hornblende from metacarbonate rocks of the Waits River Formation and its low crystallization pressure motivated us to develop a model for the Al content of calcic amphibole. Because of limited thermodynamic data for amphibole components, our model does not attempt to simulate observed amphibole compositions in the chemically complex marls. Rather, the intention of the model is to explore quantitatively, in a simple analogue system, the control of *P, T,* and coexisting mineral assemblage on amphibole composition.

Model amphibole

The composition of the amphibole samples are represented in Table 2 in terms of a single component and mole fractions of various exchange components, following the method of Thompson (1982). Tremolite [$Ca_2Mg_5Si_8O_{22}(OH)_2$] was chosen as the additive compo-

nent, and the exchange components plagioclase, edenite, and Tschermak are $CaAlNa_{-1}Si_{-1}$, $NaAlSi_1$, and $Al_2Mg_{-1}Si_{-1}$, respectively. Mole fractions of exchange components were calculated for both the 13CNK and the Fe(+2) renormalization schemes (see footnote to Table 2).

Considering the calculated mole fractions of exchange components listed in Table 2, Tschermak's component is by far the most important substitution in accounting for the Al content of the analyzed amphiboles. As a first approximation, therefore, we assumed all Al in model amphibole is incorporated by Tschermak's substitution, and the model adopted for Al-bearing calcic amphibole is a tremolite-tschermakite solid solution $[Ca_2Mg_5Si_8O_{22}(OH)_2$-$Ca_2Mg_3{}^{[6]}Al_2{}^{[4]}Al_2Si_6O_{22}(OH)_2$. In a later section, we discuss the contribution of the edenite substitution to the Al content of amphibole for selected mineral assemblages.

Activity-composition relations

Crystal structure refinements of amphiboles indicate that $^{[6]}$Al is preferentially partitioned into the M2 amphibole site (Hawthorne, 1981; Hawthorne and Grundy, 1973; Makino and Tomita, 1989). We assumed all $^{[6]}$Al resides in M2 in the model amphibole. Assuming ideal mixing and local charge balance, the activities, a, of the tremolite (tr) and tschermakite (tk) components are thus related to composition by

$$a_{tr} = (X_{MgM2})^2 \tag{1}$$

and

$$a_{tk} = (X_{AlM2})^2 \tag{2}$$

where X_{MgM2} and X_{AlM2} are the atom fractions of Mg and Al in the M2 site.

Thermodynamic data for tschermakite

An estimate of the molar volume of tschermakite at 1 bar and 298 K (267.4 cm³/mol), based on unit-cell measurements of tremolite-tschermakite solutions by X-ray diffractometry, was provided by D. M. Jenkins (personal communication, 1989). Coefficients for tschermakite in Berman's (1988) expression for heat capacity, k_0–k_3, were calculated from the following algorithm:

$$k_{i,tk} = k_{i,tr} + 2k_{i,CaAl_2SiO_6} - 2k_{i,CaMgSi_2O_6}. \tag{3}$$

Coefficients for molar volume, V_1–V_4, were calculated in an analogous fashion. Enthalpy and entropy of tschermakite at 1 bar and 298 K were estimated from (1) the compositions of tremolite-tschermakite solutions equilibrated experimentally with diopside, anorthite, and quartz (Jenkins, 1988, 1989, personal communication), and (2) the composition of amphibole coexisting with diopside, calcic plagioclase, and quartz in a calc-silicate hornfels (sample 5J of Ferry, 1989). The amphibole in the hornfels is unusually Mg rich [Mg/(Fe + Mg) = 0.98]. It closely approximates a tremolite-tschermakite solution, and is believed to have equilibrated with diopside, plagioclase, and quartz at 2000 bars and 440 ± 20 °C. At equilibrium

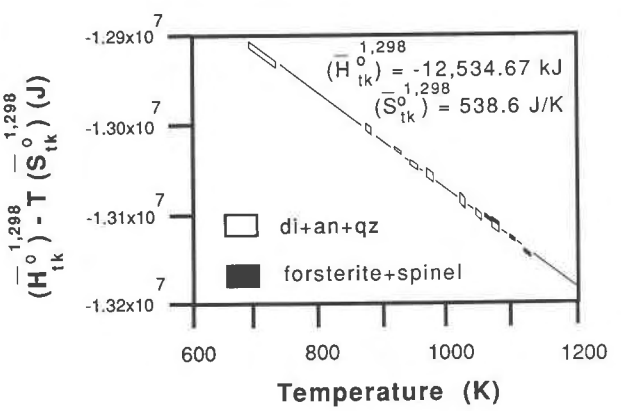

Fig. 3. Experimental data on Al content in tremolite coexisting with diopside (di), anorthite (an), and quartz (qz) (Jenkins, 1988, 1989, personal communication) and data for a calcareous hornfels from the Sierra Nevada (Ferry, 1989, sample 5J; plots at 693–733 K) were used to derive the standard state enthalpy and entropy for fictive end-member tschermakite (see text for details). $\bar{H}^0$ and $\bar{S}^0$ values were obtained from a linear regression of only the data for di + an + qz. The four data for forsterite + spinel are tentative but appear consistent with results for di + an + qz.

among the four minerals at specified P and T,

$$\bar{G}^{P,T}_{tk,am} + 2\bar{G}^{P,T}_{CaMgSi_2O_6,di} + 2\bar{G}^{P,T}_{SiO_2,qz} - \bar{G}^{P,T}_{tr,am} - 2\bar{G}^{P,T}_{CaAl_2Si_2O_8,pl} = 0. \tag{4}$$

Each of the partial molar Gibbs energy terms may be expanded:

$$\bar{G}^{P,T}_{i,j} = \bar{H}^{0\ 1,298}_{i} - T\bar{S}^{0\ 1,298}_{i} + \int_{298}^{T} C^0_i\,dT - T\int_{298}^{T}(C^0_i/T)\,dT + \int_{1}^{P}\bar{V}^0_i\,dP + RT\ln a_{i,j}. \tag{5}$$

The diopsides in Jenkins' experiments contained a small amount of Al, but because the actual compositions were not available, we assumed unit $CaMgSi_2O_6$ activity. Unit SiO_2 activity was assumed for quartz. Activity-composition relations assumed for natural diopside and plagioclase were those of Ferry (1989). Using the thermodynamic data of Berman (1988) and Equations 1–3, the only unknown terms in Equation 5 are $\bar{H}^{0\ 1,298}_{tk}$ and $\bar{S}^{0\ 1,298}_{tk}$. Considering Equation 4, each measured amphibole composition coexisting with diopside, plagioclase, and quartz at known P and T defines a value of $\bar{H}^{0\ 1,298}_{tk} - T\bar{S}^{0\ 1,298}_{tk}$. These values for all Jenkins' experimental data and for the hornfels are plotted in Figure 3 against temperature. The horizontal dimension of each rhombus corresponds to uncertainty in temperature for each datum. The temperature uncertainty for the hornfels sample (20 °C) represents the variation in T recorded by individual samples about the average temperature estimate for outcrop 5 in

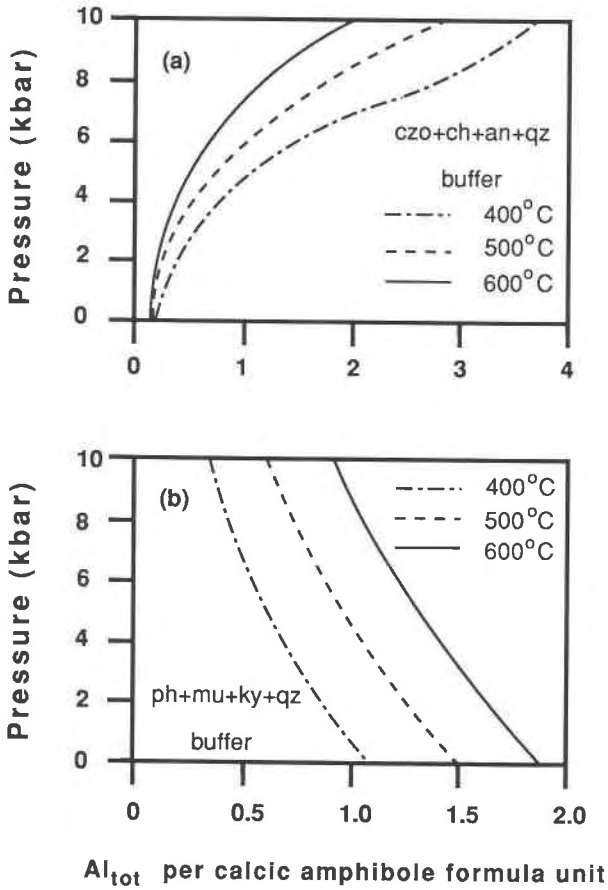

Fig. 4. Calculated total Al content, Al_{tot}, of tremolite-tschermakite amphibole as a function of P coexisting with (**a**) clinozoisite (czo) + chlorite (ch) + anorthite (an) + quartz (qz), and (**b**) phlogopite (ph) + muscovite (mu) + kyanite (ky) + quartz at 400 °C, 500 °C, and 600 °C (see text for details). Note that the Al content of amphibole and its P and T dependence are a function of P, T, and mineral assemblage.

Ferry (1989). The temperature uncertainty in the experimental data (5 °C) was taken from Jenkins (1988). The vertical dimension corresponds to uncertainty in amphibole composition. For sample 5J, the uncertainty represents the observed variation from microprobe analyses. In Jenkins' experiments, the equilibrium amphibole composition was bracketed by amphiboles that approached it from initially more Al-rich and more Al-poor compositions. For Jenkins' experimental data, the uncertainty in amphibole composition corresponds to the difference between the two bracketing compositions at each P and T. A straight line was fit to the data by linear regression of the values corresponding to the corner of each rhombus. Its slope represents our estimate for $\bar{S}^{0\,1,298}_{tk} = 538.6$ J/K·mol and its intercept our estimate for $\bar{H}^{0\,1,298}_{tk} = -12534.67$ kJ mol^{-1}. These values were derived assuming activity-composition relations (Eqs. 1 and 2) and therefore should only be applied using these same relations. Also plotted in Figure 3 are values of $\bar{H}^{0\,1,298}_{tk} - T\bar{S}^{0\,1,298}_{tk}$, derived from Jenkins' preliminary experimental data on the composition of tremolite-tschermakite solutions, equilibrated with spinel and forsterite which at equilibrium defines the following relationship:

$$\bar{G}^{P,T}_{tk,am} + 2\bar{G}^{P,T}_{Mg_2SiO_4,fo} - \bar{G}^{P,T}_{tr,am} - 2\bar{G}^{P,T}_{MgAl_2O_4,sp} = 0. \quad (6)$$

The values of $\bar{H}^{0\,1,298}_{tk} - T\bar{S}^{0\,1,298}_{tk}$ derived from these preliminary results are in good agreement with those derived from the assemblage amphibole + diopside + anorthite + quartz. The above values are different from ones derived exclusively from experimental data (Jenkins, personal communication). We included the datum for the natural sample in our analysis because without it, derived $\bar{H}^{0\,1,298}_{tk}$ and $\bar{S}^{0\,1,298}_{tk}$ values predicted undetectable amounts of Al in amphibole at $T \sim 400$–500 °C which is inconsistent with the measured composition of calcic amphibole formed during low-temperature metamorphism (e.g., Ferry, 1989). We stress, however, two points about our derived values: (1) They are, with one exception, consistent with all Jenkins' experimental data (Fig. 3). The rhombus at 918–928 K misses the calculated curve by only ~300 J. (2) They are intended to be preliminary results subject to modification by later experiment or mixing models.

Phase equilibria

General relations. For every stoichiometric reaction relationship that can be written among the components i of minerals j and the tremolite and tschermakite components of coexisting model amphibole solid solution, there exists a corresponding relationship among the partial molar Gibbs energies:

$$\sum_i \nu_i \bar{G}^{P,T}_{i,j} + \nu_{tk}\bar{G}^{P,T}_{tk,am} + \nu_{tr}\bar{G}^{P,T}_{tr,am} = 0 \quad (7)$$

where ν_i are the stoichiometric coefficients (positive for products; negative for reactants). At given P, T, and composition for all minerals except amphibole, Equations 1, 2, 5, and 7 uniquely define the composition of coexisting tremolite-tschermakite solution. These equations and Berman's (1988) thermodynamic data constitute our simple model for the Al content of calcic amphibole.

Calculated results. Results for the assemblages amphibole + anorthite + quartz + clinozoisite + chlorite and amphibole + anorthite + quartz + phlogopite + muscovite + kyanite are shown in Figure 4. The curves in Figure 4a are based on the reaction relationship

$$\begin{aligned} 14\ SiO_2 &+ 15\ Ca_2Mg_3Al_4Si_6O_{22}(OH)_2 \\ &+ 12\ Ca_2Al_3Si_3O_{12}(OH) \\ = 5\ &Ca_2Mg_5Si_8O_{22}(OH)_2 \\ &+ 4\ Mg_5Al_2Si_3O_{10}(OH)_8 \\ &+ 44\ CaAl_2Si_2O_8 \end{aligned} \quad (8)$$

while the curves in Figure 4b are based on

$$2\ KMg_3AlSi_3O_{10}(OH)_2 + 10\ SiO_2 + 3\ Ca_2Mg_3Al_4Si_6O_{22}(OH)_2 = 3\ Ca_2Mg_5Si_8O_{22}(OH)_2 + 2\ KAl_3Si_3O_{10}(OH)_2 + 4\ Al_2SiO_5. \quad (9)$$

In Figure 4, Al_{tot} (total Al atoms in amphibole pfu) is $4(X_{AlM2})$ in Equation 2. Calculated results lead to three conclusions: (1) Even at a given P and T in the simple model system, the Al content of calcic amphibole is critically dependent on the coexisting mineral assemblage. (2) There is no universal relationship, either quantitative or qualitative, between pressure and the Al content of calcic amphibole. With increasing pressure at constant temperature, the Al content of amphibole coexisting with anorthite, quartz, clinozoisite, and chlorite increases, but it decreases in amphibole in equilibrium with anorthite, quartz, phlogopite, muscovite, and kyanite. (3) The Al content of amphibole, even in equilibrium with a given mineral buffer assemblage, may vary as a function of T as well as P.

We systematically considered equilibrium among tremolite-tschermakite amphibole and anorthite, quartz, clinozoisite, chlorite, phlogopite, kyanite, diopside, muscovite, potassium feldspar, calcite, and dolomite in the system K_2O-CaO-MgO-Al_2O_3-SiO_2-H_2O-CO_2. Because calcic amphibole from the Waits River Formation coexists with plagioclase and quartz, we restricted our attention to assemblages with anorthite + quartz. Further, equilibria with CO_2-H_2O-bearing fluid were not considered. Because of the interest in the Al content in amphibole as a geobarometer, results are presented in Figure 5a on an isothermal P-Al_{tot} diagram. Unit activity was assumed for components, except amphibole, in all minerals. The arrangement of univariant curves in Figure 5a is consistent with the method of Schreinemakers. The shapes of the curves in Figure 5a are robust because they depend only on $\Delta\bar{V}$ and the stoichiometry of the reaction relationship. Qualitatively the shapes are independent of entropies and enthalpies of reaction. Equilibria in some parts of Figure 5a are metastable relative to a CO_2-H_2O fluid. At 525 °C the assemblage amphibole + anorthite + quartz is stable up to ~9000 bars, and amphibole contains ~0.2–1.2 Al atoms pfu depending on P and coexisting minerals. Figure 5b shows the compatibility of minerals in the divariant regions of Figure 5a on a diagram that projects through $Ca_2Mg_5Si_8O_{22}(OH)_2$, $Ca_2Mg_3Al_4Si_6O_{22}(OH)_2$, $CaAl_2Si_2O_8$, and SiO_2 (i.e., considering only assemblages that coexist with tremolite-tschermakite amphibole, anorthite, and quartz). The projection scheme in Figure 5b was derived from a transformation of components (see Thompson, 1982). The arrows pointing outward from the triangles emphasize that tie lines between kyanite and other minerals first pass to infinity and then return to the CaO apex of the diagram (cf. tie lines to potassium feldspar on the Thompson AFM diagram, Thompson, 1957). The tie lines between chlorite or clinozoisite and other minerals pass directly from the CaO apex into the interior of the diagram.

Discussion of calculated results. Calculated results in Figure 5a are in qualitative agreement with a number of observations on the natural occurrence of Al-bearing calcic amphibole coexisting with plagioclase and quartz: (1) The least aluminous amphibole samples are from diopside-bearing rocks (Fig. 2b). (2) Calcic amphibole coexisting with more aluminous mineral such as micas, chlorite, clinozoisite, and aluminum silicate is more aluminous (Table 2; Fig. 2a). (3) Calcic amphiboles may be relatively aluminous even when they coexist with calcite and dolomite (Table 2). (4) Calcic amphibole coexists with kyanite (kyanite is metastable below $P \sim 4.2$ kbars) only at elevated pressure (fields 3–8 and 13, Fig. 5a); such amphibole is the most aluminous possible coexisting with plagioclase and quartz (cf. Selverstone et al., 1984). The good qualitative agreement between natural amphibole occurrences and the mineral relationships predicted by the simple model in Figure 5a further emphasizes that both the Al content of calcic amphibole and its pressure dependence are critically dependent on coexisting minerals.

Shortcomings of the simple thermodynamic model

The thermodynamic model for Al substitution in calcic amphibole predicts an Al content of ~0.4–1.0 atoms pfu in amphibole coexisting with anorthite + quartz at the P-T conditions of metamorphism of the Waits River Formation, northern Vermont (3500 bars, 525 °C). Measured amphibole compositions are much more aluminous (Table 2). Analyses in Table 2 show that a positive correlation exists between the Na and Al contents of calcic amphibole. In addition, Figure 2 demonstrates that, empirically, high Al content in amphibole is correlated with high (Fe + Mn)/(Fe + Mg + Mn). Quantitatively, therefore, it appears that a major shortcoming of the simple model is its failure to incorporate Na and Fe.

Edenite substitution and the Al content of amphibole

The mole fractions of exchange components in Table 2 demonstrate that there is significant Na in natural Al-rich amphibole and that Na in amphibole is largely accommodated by the edenite substitution. Potentially the edenite substitution could explain why natural amphibole contains more Al than predicted by our simple model for a Na-free system. We therefore investigated the edenite content of amphibole and its contribution to Al_{tot} for the same two assemblages represented in Figure 4. Amphibole with tremolite, tschermakite, and edenite solutions coexists with plagioclase solutions rather than pure anorthite. To calculate the edenite content of such amphibole, we used the following stoichiometric reaction relationship among albite, tremolite, and edenite components and quartz:

$$NaAlSi_3O_8 + Ca_2Mg_5Si_8O_{22}(OH)_2 = NaCa_2Mg_5Si_7AlO_{22}(OH)_2 + 4\ SiO_2 \quad (10)$$

and these activity-composition relations:

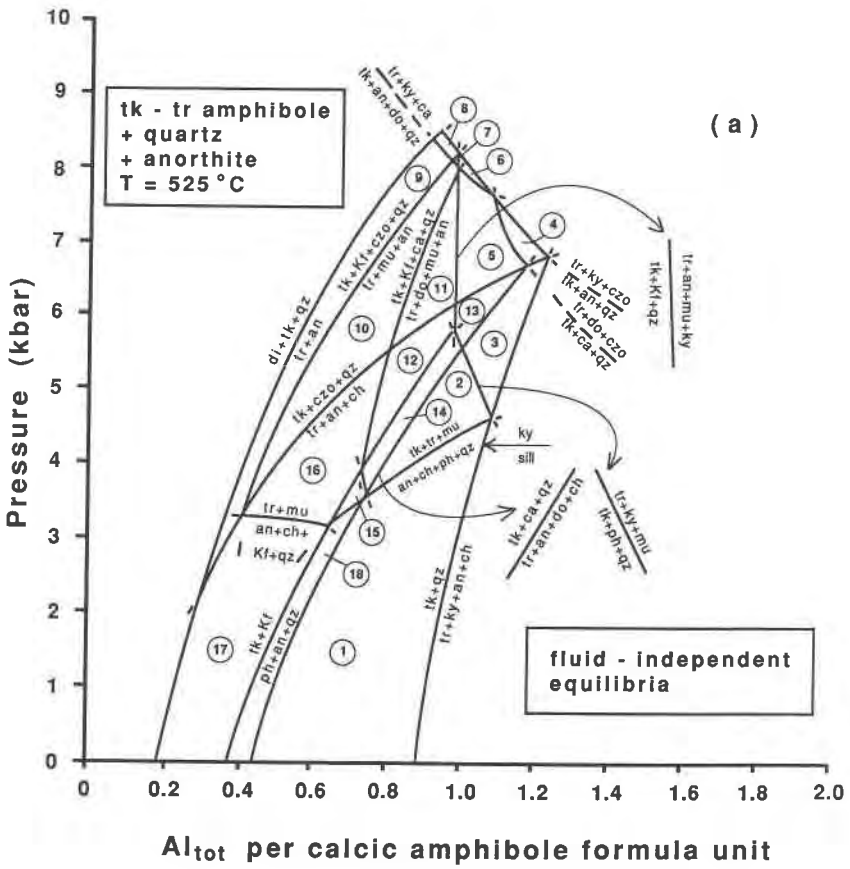

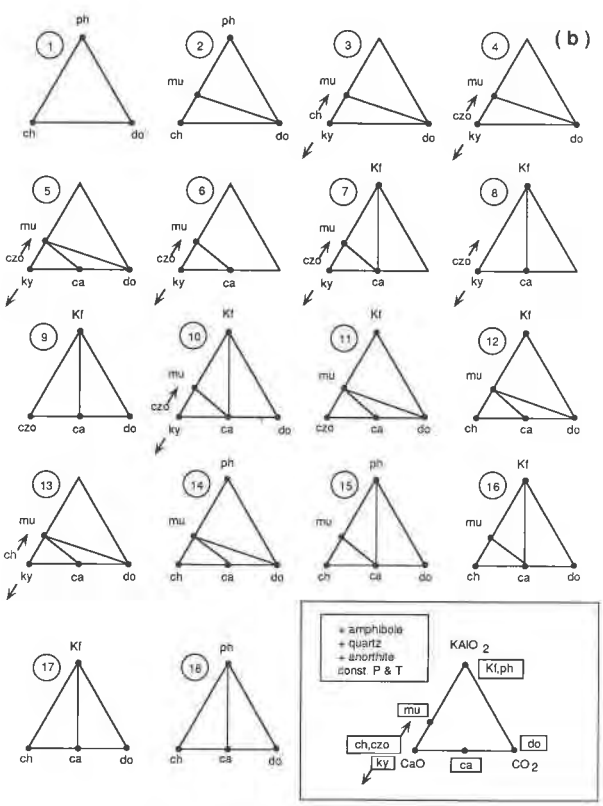

Fig. 5. (**a**) Calculated total Al content, Al_{tot}, of tremolite-tschermakite amphibole as a function of P at 525 °C coexisting with selected mineral assemblages in the system K_2O-CaO-MgO-Al_2O_3-SiO_2-H_2O-CO_2 (see text for details). All assemblages contain anorthite + quartz. Kyanite is metastable below $P \sim 4.2$ kbar. Mineral abbreviations as in Figure 4; ca = calcite; do = dolomite; Kf = potassium feldspar; sill = sillimanite. Circled numbers identify divariant regions with mineral compatibilities shown in *b*. Note that the Al content of amphibole and its P dependence critically depend on the coexisting mineral assemblage. (**b**) Compatibility of minerals in the divariant regions of **a** on a diagram that projects through $Ca_2Mg_5Si_8O_{22}(OH)_2$, $Ca_2Mg_3Al_4Si_6O_{22}(OH)_2$, $CaAl_2Si_2O_8$, and SiO_2 (i.e., considering only assemblages that contain tremolite-tschermakite amphibole, anorthite, and quartz).

$$a_{ed} = (1 - X_{V,A})(X_{MgM2})^2 \quad (11)$$

$$a_{tr} = (X_{V,A})(X_{MgM2})^2 \quad (12)$$

$$a_{tk} = (X_{V,A})(X_{AlM2})^2 \quad (13)$$

where $X_{V,A}$ is the atom fraction of vacancies in the amphibole A-site. We used the thermodynamic data base of Holland and Powell (1990) for these calculations because Berman's (1988) data base does not include edenite. The activity coefficients for $CaAl_2Si_2O_8$ and $NaAlSi_3O_8$ in plagioclase were taken as 2 and 1, respectively (Carpenter and Ferry, 1984). For a specified T and a_{an}, $X_{V,A}$ may be determined from Equations 5, 7, and 10–12. Values for

$X_{V,A}$ are then included in the tremolite and tschermakite activity terms (Eqs. 12 and 13); values for X_{MgM2} and X_{AlM2} are finally calculated using Equations 5, 7, 12, and 13. Al_{tot} for tremolite-tschermakite-edenite amphibole is $(1 - X_{V,A}) + 4(1 - X_{MgM2})$.

Calculated results (Fig. 6) show that the Al content of tremolite-tschermakite-edenite amphibole solutions can significantly differ from that of tremolite-tschermakite amphibole solutions depending on the extent of the edenite substitution as controlled by the composition of coexisting plagioclase (by Reaction 10). For equilibria that do not involve the anorthite component, such as phlogopite-muscovite-kyanite-quartz-plagioclase-amphibole (Reactions 9 and 10), increasing edenite substitution (i.e., increasing a_{ab}) results in an increase in the Al content of amphibole (Fig. 6b). In general, however, the increase is small ($\leq$0.5 Al pfu) and inadequate to explain the very high Al content of the amphibole analyzed. For equilibria that involve the anorthite component, such as clinozoisite-chlorite-plagioclase-quartz-amphibole (Reactions 8 and 10), however, increasing edenite substitution actually results in a reduction in the Al content of amphibole (Fig. 6a). The reduction in Al_{tot} occurs because the effect of an increase in edenite content caused by increasing a_{ab} is offset by a decrease in tschermakite content caused by decreasing a_{an}. Consideration of Na substitution in amphibole by the edenite substitution, therefore, fails to explain the discrepancy between the Al content of analyzed amphiboles and that predicted by the model.

Calculated results in Figure 6a nevertheless provide a simple thermodynamic model for the difference in Al content of calcic amphibole between mafic greenschists and amphibolites. Mafic greenschists and amphibolites typically contain the same mineral assemblage (clinozoisite + chlorite + plagioclase + quartz + calcic amphibole). Greenschists, however, contain Na-rich plagioclase and Al-poor actinolite, while amphibolites contain calcic plagioclase and Al-rich hornblende (Laird, 1982). The correlation between Na-rich plagioclase and Al-poor amphibole and between calcic plagioclase and Al-rich amphibole is the result of the dependence of the edenite and tschermakite contents of amphiboles with tremolite, tschermakite, and edenite solutions, coexisting with chlorite, clinozoisite, quartz, and plagioclase, on the plagioclase composition.

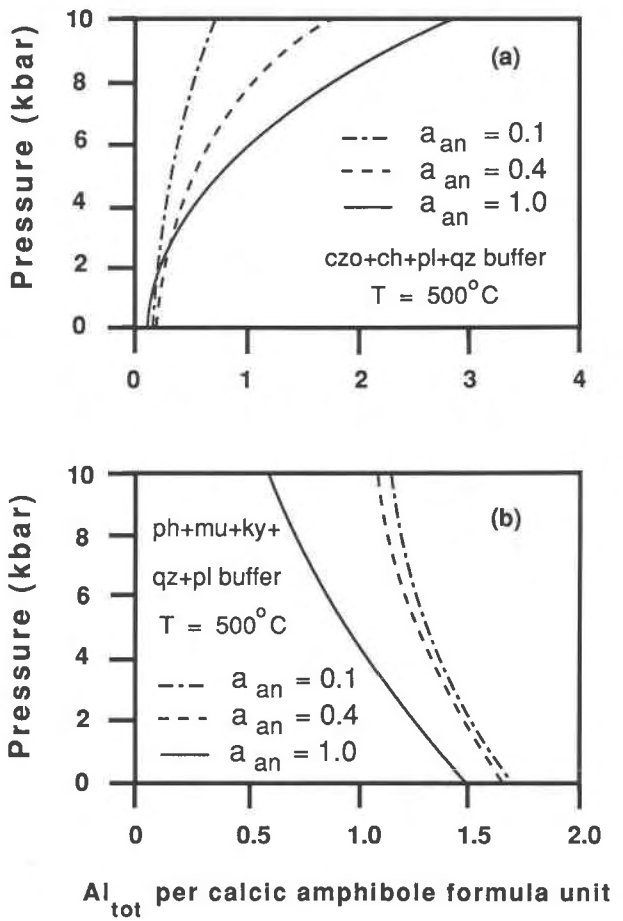

Fig. 6. Calculated total Al content, Al_{tot}, of tremolite-tschermakite-edenite amphibole coexisting with the same mineral assemblages as in Figure 4 as a function of a_{an} for a_{an} = 0.1, 0.4, and 1.0 (see text for details).

Fe-Mg substitution and the Al content of amphibole

We verified that Fe-Mg substitution has an effect on the Al content of calcic amphibole by deriving expressions for the relationship between the chemical potential of an aluminous component of calcic amphibole (μ_{Alam}) and the Fe/(Fe + Mg) of coexisting minerals i (X_{Fei}) using the Gibbs method (Spear et al., 1982). The composition of coexisting Fe-Mg minerals indirectly monitors Fe-Mg substitution in amphibole. Two assemblages relevant to metamorphosed marls from the Waits River Formation were considered, amphibole + plagioclase + quartz + chlorite + clinozoisite and amphibole + plagioclase + quartz + chlorite + calcite + ankerite. In both cases Fe/(Fe + Mg) in chlorite was used to monitor Fe-Mg substitution in amphibole. Table 4 contains the components used to model the compositions of the minerals and the linearly independent stoichiometric reaction relationships that can be written among components in each assemblage. The Gibbs method was used to derive expressions for $(\partial\mu_{Alam}/\partial X_{Fech})$ at conditions of constant pressure, temperature, and composition of coexisting plagioclase and clinozoisite by solving a set of differential equations that includes a Gibbs-Duhem equation for each phase and the differentials of the conditions of heterogeneous equilibrium implied by the reaction relationships in Table 4 (see Spear et al., 1982 for further details). Ideal mixing of the Fe and Mg components in the chlorite solid solution was assumed. Results are presented in Table 4. Using measured mineral compositions (Table 2) and an inferred temperature of metamorphism of 525 °C, values of $(\partial\mu_{Alam}/\partial X_{Fech})_{P,T,X_{an},X_{czo}}$ were computed for three samples of impure carbonate rock from the Waits River Formation (Table 4). All calculated values are positive. Al-

TABLE 4. Prediction of Al-Fe correlation in amphibole by the Gibbs method

Components used to model compositions of minerals

Mineral	Symbol	Formula	Method for computing Xi from ineral analyses
amphibole (amp)	Feam	$Ca_2Fe_5Si_8O_{22}(OH)_2$	$X_{Feam} = Fe/(Fe + Mg + {}^{[6]}Al)$
	Mgam	$Ca_2Mg_5Si_8O_{22}(OH)_2$	$X_{Mgam} = Mg/(Fe + Mg + {}^{[6]}Al)$
	Alam	$Ca_2Al_{10}Si_3O_{22}(OH)_2$	$X_{Alam} = {}^{[6]}Al/(Fe + Mg + {}^{[6]}Al)$
chlorite (ch)	Fech	$Fe_5Al_2Si_3O_{10}(OH)_8$	$X_{Fech} = Fe/(Fe + Mg)$
	Mgch	$Mg_5Al_2Si_3O_{10}(OH)_8$	$X_{Mgch} = Mg/(Fe + Mg)$
dolomite (do)	Fedo	$CaFe(CO_3)_2$	$X_{Fedo} = Fe/(Fe + Mg)$
	Mgdo	$CaMg(CO_3)_2$	$X_{Mgdo} = Mg/(Fe + Mg)$
clinozoisite (czo)	Feczo	$Ca_2Fe_3Si_3O_{12}(OH)$	$X_{Feczo} = Fe^{3+}/(Fe^{3+} + Al)$
	Alczo	$Ca_2Al_3Si_3O_{12}(OH)$	$X_{Alczo} = Al/(Fe^{3+} + Al)$
plagioclase (pl)	an	$CaAl_2Si_2O_8$	$X_{an} = Ca/(Ca + Na)$
	ab	$NaAlSi_3O_8$	$X_{ab} = Na/(Ca + Na)$
calcite (ca)	ca	$Ca(CO_3)$	
quartz (qa)	qz	SiO_2	

Reaction relationships

1. Exchange reactions
   1 Feam + 1 Mgch = 1 Fech + 1 Mgam
   5 Fedo + 1 Mgam = 5 Mgdo + 1 Feam
2. Net-transfer reactions
   2 Mgch + 22 an = 3 Alam + 2 Mgam + 6 Alczo + 7 qz
   5 Mgch + 15 Mgdo + 55 an = 12 Alam + 8 Mgam + 30 ca + 25 qz

System of equations in matrix form for the equilibrium

1. amp + ch + ca + do + qz + pl

$$\begin{bmatrix} X_{Fech} & X_{Mgch} & 0 & 0 & 0 & 0 & 0 \\ 0 & 0 & X_{Fedo} & X_{Mgdo} & 0 & 0 & 0 \\ 0 & 0 & 0 & 0 & X_{Feam} & X_{Mgam} & X_{Alam} \\ 1 & -1 & 0 & 0 & -1 & 1 & 0 \\ 0 & 0 & -5 & 5 & 1 & -1 & 0 \\ 0 & -5 & 0 & -15 & 0 & 8 & 12 \\ -1 & 1 & 0 & 0 & 0 & 0 & 0 \end{bmatrix} \begin{bmatrix} \partial\mu_{Fech}/\partial X_{Fech} \\ \partial\mu_{Mgch}/\partial X_{Fech} \\ \partial\mu_{Fedo}/\partial X_{Fech} \\ \partial\mu_{Mgdo}/\partial X_{Fech} \\ \partial\mu_{Feam}/\partial X_{Fech} \\ \partial\mu_{Mgam}/\partial X_{Fech} \\ \partial\mu_{Alam}/\partial X_{Fech} \end{bmatrix} = \begin{bmatrix} 0 \\ 0 \\ 0 \\ 0 \\ 0 \\ 0 \\ -Gxx \end{bmatrix}$$

2. amp + ch + czo + qz + pl

$$\begin{bmatrix} X_{Fech} & X_{Mgch} & 0 & 0 & 0 \\ 0 & 0 & X_{Feam} & X_{Mgam} & X_{Alam} \\ 1 & -1 & -1 & 1 & 0 \\ 0 & -2 & 0 & 2 & 3 \\ -1 & 1 & 0 & 0 & 0 \end{bmatrix} \begin{bmatrix} \partial\mu_{Fech}/\partial X_{Fech} \\ \partial\mu_{Mgch}/\partial X_{Fech} \\ \partial\mu_{Feam}/\partial X_{Fech} \\ \partial\mu_{Mgam}/\partial X_{Fech} \\ \partial\mu_{Alam}/\partial X_{Fech} \end{bmatrix} = \begin{bmatrix} 0 \\ 0 \\ 0 \\ 0 \\ -Gxx \end{bmatrix}$$

where $G_{xx} = (\partial^2 G_{ch}/\partial X^2_{Fech})_{P,T} = 5RT/X_{Fech}X_{Mgch}$

Values of $\partial\mu_{Alam}/\partial X_{Fech}$ for three different amphibole-zone specimens from the Waits River Formation, northeastern Vermont in joules

Sample number	X_{Fech}	X_{Fedo}	X_{Feam}	X_{Mgam}	$(\partial\mu_{Alam}/\partial X_{Fech})_{P,T,X_{an}}$ amp − pl − qz − ca − ch − do	$(\partial\mu_{Alam}/\partial X_{Fech})_{P,T,X_{an},X_{czo}}$ amp − pl − qz − ch − czo
57-13A	0.27	0.19	0.26	0.61	7334	—
56-4C	0.48	0.28	0.37	0.39	9185	768
56-11	0.55	—	0.41	0.29	—	4468

though it is not possible to simply relate μ_{Alam} quantitatively to the Al content of calcic amphibole in atoms pfu, the Gibbs method indeed predicts that substitution of Fe for Mg in amphibole results in elevated Al contents. The results in Table 4 were obtained by consideration of mineral equilibrium in individual samples. The results demonstrate that the Fe-Al correlation in amphibole illustrated in Figure 2 should have been anticipated.

The positive correlation between the Fe and Al content of calcic amphibole is probably, in part, the result of Fe-Mg ordering among the M1, M2, and M3 crystallographic sites in amphibole. Crystal structure refinements of amphibole indicate that Fe is partitioned into the M1 and M3 sites preferentially over the M2 site (e.g., Hawthorne, 1981; Makino and Tomita, 1989). For example, Makino and Tomita (1989) estimated that even in calcic amphibole that crystallized at high temperature in granulites and volcanic rocks, $K_d^{M1\text{-}M2} = (Mg/Fe)_{M1}/(Mg/Fe)_{M2} = 0.3$. Amphiboles that crystallized at lower temperatures, like those in marls from the Waits River Formation, probably are characterized by $K_d^{M1\text{-}M2} \ll 0.3$.

The effect of Fe-Mg ordering among the amphibole M sites on the Al content of calcic amphibole can be seen by considering the specific case of coexisting amphibole $[Ca_2(Fe,Mg)_3(Al,Fe,Mg)_2(Al,Si)_8O_{22}(OH)_2]$, chlorite $[(Fe,Mg)_5Al_2Si_3O_{10}(OH)_8]$, ankerite $[Ca(Fe,Mg)(CO_3)_2]$, calcite $[Ca(CO_3)]$, anorthite $[CaAl_2Si_2O_8]$, and quartz $[SiO_2]$. The following reaction relationship can be written among the Fe-free mineral components:

$$6\ Ca_2Mg_3Al_4Si_6O_{22}(OH)_2 + 6\ CaCO_3 + 5\ SiO_2 = 2\ Ca_2Mg_5Si_8O_{22}(OH)_2 + 3\ CaMg(CO_3)_2 + 11\ CaAl_2Si_2O_8 + Mg_5Al_2Si_3O_{10}(OH)_8. \quad (14)$$

At equilibrium (assuming ideal mixing, local charge balance, and identical site occupancies of M1 and M3), Equation 14 implies an equilibrium constant,

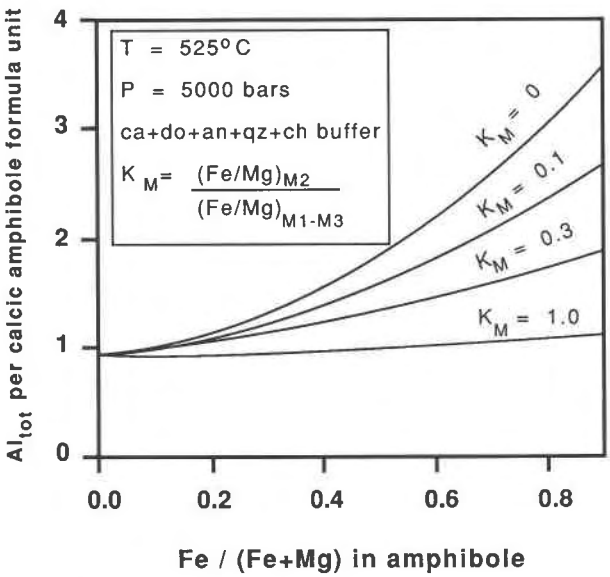

Fig. 7. Calculated dependence of the Al content of tremolite-tschermakite amphibole, Al_{tot}, coexisting with calcite + dolomite + anorthite + chlorite + quartz at 525 °C, 5000 bars on Fe/Fe + Mg in amphibole. See text for details. Note that the dependence of Al_{tot} on Fe/Fe + Mg depends critically on K_m, a measure of the partitioning of Fe and Mg between the M1, M2, and M3 sites in amphibole.

$$K_{eq} = \frac{(X^{6}_{Mg,M1-M3})(X^{4}_{Mg,M2})(X^{3}_{Mg,ank})(X^{5}_{Mg,ch})}{(X^{18}_{Mg,M1-M3})(X^{12}_{Al,M2})} \qquad (15)$$

where the X_i terms refer to the atom fraction of i in the appropriate site. Using the thermodynamic data for tschermakite in this study and for the other Fe-free mineral components in Berman (1988) at 525 °C, 5 kbar,

$$K'_{eq} = (K_{eq})^{1/4}$$

$$= \frac{(X_{Mg,M2})(X^{3/4}_{Mg,ank})(X^{5/4}_{Mg,ch})}{(X^{3}_{Mg,M1-M3})(X^{3}_{Al,M2})} = 62.387. \qquad (16)$$

Partitioning of Fe and Mg between the M1−M3 and M2 sites is quantitatively described by

$$K_m = \frac{(Mg/Fe)_{M1-M3}}{(Mg/Fe)_{M2}}. \qquad (17)$$

The bulk Fe-Mg partition coefficients for chlorite and amphibole and for ankerite and amphibole were estimated from the composition of coexisting minerals in sample 56-4C:

$$K_d^{am\text{-}ch} = (Fe/Mg)_{am}/(Fe/Mg)_{ch} = 1.06 \qquad (18)$$

$$K_d^{am\text{-}ank} = (Fe/Mg)_{am}/(Fe/Mg)_{ank} = 2.42. \qquad (19)$$

For a specified value of K_m and Fe/(Fe + Mg) in amphibole, the Al content of calcic amphibole can be computed from Equations 1, 2, and 16–19. Results are illustrated in Figure 7 for representative regional metamorphic *P-T* conditions and for four values of K_m. It is not simply the substitution of Fe for Mg that results in elevated Al contents in amphibole because if Fe and Mg mix randomly over the M1, M2, and M3 sites (K_m = 1), Fe-Mg substitution has a negligible effect on Al_{tot}. The simple analysis shows that substitution of Fe for Mg in calcic amphibole only results in a dramatic increase in its Al content when Fe shows a strong preference for the M1 and M3 sites over the M2 sites (i.e., K_m < 0.3). The effect may be greater if Fe-Mg mixing is nonideal.

Consideration of edenite substitution (Fig. 6), Fe-Mg substitution, and Fe-Mg ordering in amphibole (Fig. 7) fails to reproduce the Al contents of natural calcic amphibole (Table 2). These results demonstrate that before the Al content of amphibole can generally be used as a geothermobarometer, much remains to be learned about the thermodynamic properties of amphibole solid solutions. Our study suggests that, as a beginning, the correlation between Fe and Al contents in calcic amphibole must be calibrated either empirically or experimentally in the laboratory. Experiments should include not only studies of $Ca_2Fe_5Si_8O_{22}(OH)_2$-$Ca_2Fe_3Al_4Si_6O_{22}(OH)_2$ solid solutions but also of the partitioning of Fe and Mg among amphibole M sites.

Conclusions

Microprobe analyses reveal that calcic amphibole, crystallized at the same metamorphic grade in carbonate rocks from northern Vermont, has a great range in Al content, 0.38–3.30 atoms pfu. The metacarbonates are interbedded with andalusite-bearing schists. These results lead to three conclusions: (1) High-Al amphibole is not restricted to high-pressure metamorphic environments, because the amphiboles from Vermont are some of the most aluminous ever reported and yet crystallized at P < 3800 bars. (2) High-Al amphiboles is not restricted to highly aluminous rocks, because the amphiboles from Vermont crystallized in carbonate rocks with <15 wt% Al_2O_3. (3) The Al content of calcic amphibole is not just a function of pressure, but also of temperature, mineral assemblage, composition of coexisting minerals [principally Fe/(Fe + Mg) and plagioclase composition], and partitioning of Fe and Mg among the M1, M2, and M3 amphibole crystallographic sites.

Acknowledgments

Acknowledgment is made to the National Science Foundation (grant EAR-8903493 to J.M.F.) and to the donors of the Petroleum Research Fund, administered by the American Chemical Society, for this research. Microprobe analyses were obtained with an instrument partially funded by NSF grant EAR-8606864. Field work by A.L. was made possible in part by financial support from the Geological Society of America, Sigma Xi, and the Department of Earth and Planetary Sciences at The Johns Hopkins University. We thank Eugene Smelik for his examination of some amphibole samples with the transmission electron microscope. This study could not have been possible without David M. Jenkins who kindly supplied us with his experimental data prior to publication. Jenkins' experimental program was supported by NSF grant EAR-8803437. We warmly thank J.B. Thompson, Jr., for introducing us to many of his enthusiasms that we utilized in this research: the crystal chemistry of amphiboles, the thermodynamic properties of minerals, Schreinemakers analysis, projected phase diagrams, and the Gibbs method. The manuscript was improved by helpful reviews from M. Cho and C.R. Nabelek.

References cited

Anovitz, L.M., and Essene, E.J. (1987) Phase equilibria in the system $CaCO_3$-$MgCO_3$-$FeCO_3$. Journal of Petrology, 28, 389–414.

Berman, R.G. (1988) Internally-consistent thermodynamic data for minerals in the system Na_2O-K_2O-CaO-MgO-FeO-Fe_2O_3-Al_2O_3-SiO_2-TiO_2-H_2O-CO_2. Journal of Petrology, 29, 445–522.

Cady, W.M. (1960) Stratigraphic and geotectonic relationships in northern Vermont and southern Quebec. Geological Society of America Bulletin, 71, 531–576.

Cao, R., Ross, C., and Ernst, W.G. (1986) Experimental studies to 10 kb of the bulk composition $tremolite_{50}$ – $tschermakite_{50}$ + excess H_2O. Contributions to Mineralogy and Petrology, 93, 160–167.

Carpenter, M.A., and Ferry, J.M. (1984) Constraints on the thermodynamic mixing properties of plagioclase feldspars. Contributions to Mineralogy and Petrology, 87, 138–148.

Dennis, J.G. (1956) The geology of the Lyndonville area, Vermont. Vermont Geological Survey Bulletin, 8, 98 p.

Doll, C.G. (1951) Geology of the Memphremagog quadrangle and the southeastern portion of the Irasburg quandrangle, Vermont. Vermont Geological Survey Bulletin, 3, 113 p.

Doll, C.G., Cady, W.M., Thompson, J.B., Jr., and Billings, M.P. (1961) Centennial geologic map of Vermont. Vermont Geological Survey, Burlington, Vermont.

Doolan, B.L., Zen, E., and Bence, A.E. (1978) Highly aluminous hornblendes: Compositions and occurrences from southwestern Massachusetts. American Mineralogist, 63, 1088–1099.

Eric, J.H., and Dennis, J.G. (1958) Geology of the Concord-Waterford area, Vermont. Vermont Geological Survey Bulletin, 11, 66 p.

Ferry, J.M. (1989) Contact metamorphism of roof pendants at Hope Valley, Alpine County, California, USA: A record of the hydrothermal system of the Sierra Nevada batholith. Contributions to Mineralogy and Petrology, 101, 402–417.

Ferry, J.M., and Spear, F.S. (1978) Experimental calibration of the partitioning of Fe and Mg between biotite and garnet. Contributions to Mineralogy and Petrology, 66, 113–117.

Hall, L.M. (1959) The geology of the St. Johnsbury quadrangle, Vermont and New Hampshire. Vermont Geological Survey Bulletin, 13, 105 p.

Hammarstrom, J.M., and Zen, E. (1986) Aluminum in hornblende: An empirical igneous geobarometer. American Mineralogist, 71, 1297–1313.

Hawthorne, F.C. (1981) Crystal chemistry of the amphiboles. In Mineralogical Society of America Reviews in Mineralogy, 9A, 1–102.

Hawthorne, F.C., and Grundy, H.D. (1973) The crystal chemistry of the amphiboles. I. Refinement of the crystal structure of ferrotschermakite. Mineralogical Magazine, 39, 36–48.

Hodges, K.V., and Spear, F.S. (1982) Geothermometry, geobarometry and the Al_2SiO_5 triple point at Mt. Moosilauke, New Hampshire. American Mineralogist, 67, 1118–1134.

Holdaway, M.J. (1971) Stability of andalusite and the aluminum silicate phase diagram. American Journal of Science, 271, 97–131.

Holland, T.J.B., and Powell, R. (1990) An enlarged and updated internally consistent thermodynamic dataset with uncertainties and correlations: The system K_2O-Na_2O-CaO-MgO-MnO-FeO-Fe_2O_3-Al_2O_3-TiO_2-SiO_2-C-H_2-O_2. Journal of Metamorphic Geology, 8, 89–124.

Hollister, L.S., Grissom, G.C., Peters, E.K., Stowell, H.H., and Sisson, V.B. (1987) Confirmation of the empirical correlation of Al in hornblende with pressure of solidification of calk-alkaline plutons. American Mineralogist, 72, 231–239.

Jenkins, D.M. (1988) Experimental study of the join tremolite-tschermakite: A reinvestigation. Contributions to Mineralogy and Petrology, 99, 392–400.

——— (1989) Experimental reversal of the Al content of tremolitic amphiboles coexisting with diopside, anorthite, and quartz. Geological Society of America Abstract with Programs, 21, A157.

Johnson, M.C., and Rutherford, M.J. (1989a) Experimental calibration of the aluminum-in-hornblende geobarometer with application to Long Valley caldera (California) volcanic rocks. Geology, 17, 837–841.

——— (1989b) Experimentally determined conditions in the Fish Canyon Tuff, Colorado, magma chamber. Journal of Petrology, 30, 711–738.

Konig, R.H., and Dennis, J.G. (1964) The geology of the Hardwick area, Vermont. Vermont Geological Survey Bulletin, 24, 57 p.

Kostyuk, E.A., and Sobolev, V.S. (1969) Paragenetic types of calciferous amphiboles of metamorphic rocks. Lithos, 2, 67–81.

Laird, J. (1982) Amphiboles in metamorphosed basaltic rocks: Greenschist facies to amphibolite facies. In Mineralogical Society of America Reviews in Mineralogy, 9B, 113–137.

Leake, B.E. (1965a) The relationship between tetrahedral aluminum and the maximum possible octahedral aluminum in natural caciferous and subcaliferous amphiboles. American Mineralogist, 50, 843–851.

——— (1965b) The relationship between composition of calciferous amphibole and grade of metamorphism. In W.S. Pitcher and G.W. Flinn, Eds., Controls of metamorphism, p. 299–318. Wiley, New York.

——— (1971) On aluminous and edenitic hornblendes. Mineralogical Magazine, 38, 389–407.

——— (1978) Nomenclature of amphiboles. American Mineralogist, 63, 1023–1052.

Makino, K., and Tomita, K. (1989) Cation distribution in the octahedral sites of hornblendes. American Mineralogist, 74, 1097–1105.

Pluysnina, L.P. (1982) Geothermometry and geobarometry of plagioclase-hornblende bearing assemblages. Contributions to Mineralogy and Petrology, 80, 140–146.

Powneby, M.I., Wall, V.J., and O'Neill, H.St.C. (1987) Fe-Mn partitioning between garnet and ilmenite: Experimental calibration and applications. Contributions to Mineralogy and Petrology, 97, 116–126.

Raase, P. (1974) Al and Ti contents of hornblende, indicators of pressure and temperature of regional metamorphism. Contributions to Mineralogy and Petrology, 45, 231–236.

Robinson, P., and Jaffe, H.W. (1969) Chemographic exploration of amphibole assemblages from central Massachusetts and southwestern New Hampshire. Mineralogical Society of America Special Paper 2, 251–274.

Sawaki, T. (1989) Sadanagaite and subsilicic ferroan pargasite from thermally metamorphosed rocks in the Nogo-Hakusan area, central Japan. Mineralogical Magazine, 53, 99–106.

Selverstone, J., Spear, F.S., Franz, G., and Morteani, G. (1984) High-pressure metamorphism in the SW Tauern Window, Austria: P-T paths from hornblende-kyanite-staurolite schists. Journal of Petrology, 25, 501–531.

Spear, F.S. (1981) An experimental study of hornblende stability and compositional variability in amphibolite. American Journal of Science, 281, 697–734.

Spear, F.S., Ferry, J.M., and Rumble, D., III. (1982) Analytical formulation of phase equilibria: The Gibbs' method. In Mineralogical Society of America Reviews in Mineralogy, 10, 105–206.

Thompson, J.B., Jr. (1957) The graphical analysis of mineral assemblages in pelitic schists. American Mineralogist, 42, 842–858.

——— (1982) Compositional space: An algebraic and geometric approach. In Mineralogical Society of America Reviews in Mineralogy, 10, 1–51.

Thompson, J.B., Jr., and Norton, S.A. (1968) Paleozoic regional metamorphism in New England and adjacent areas. In E-an Zen, W.S. White, J.B. Hardley, and J.B. Thompson, Jr., Eds., Studies of Appalachian geology—Northern and maritime, p. 203–218. Interscience Publishers, New York.

Woodland, B.G. (1965) The geology of the Burke quadrangle, Vermont. Vermont Geological Survey Bulletin, 28, 151 p.

Manuscript received January 5, 1990
Manuscript accepted March 1, 1991

APPENDIX TABLE 1. Biotite-garnet, calcite-dolomite, and ilmenite-garnet geothermometry for 18 samples from the Waits River Formation, northern Vermont

	Mineral composition data										Calculated temperatures			
Sample	Xal, ga	Xpy, ga	Xsp, ga	Xgr, ga	XFe, bi	XMg, bi	XFe, il	XMn, il	XFe, ca	XMg, ca	G-B*	G-B**	G-I†	C-D‡
48-1	0.758	0.082	0.113	0.047	0.519	0.481					451	469		
48-1A	0.712	0.121	0.031	0.137	0.459	0.541	0.994	0.006			508	560	551	
48-1B	0.764	0.115	0.023	0.099	0.490	0.510					508	546		
48-2A	0.680	0.102	0.082	0.135	0.502	0.498	0.968	0.032			522	573		
48-34	0.671	0.082	0.044	0.204	0.477	0.523	0.992	0.008			440	513	517	
49-1A	0.580	0.080	0.100	0.240	0.500	0.500					495	583		
49-1B	0.534	0.061	0.139	0.266	0.517	0.483					459	558		
56-4A	0.541	0.095	0.126	0.238	0.408	0.592	0.972	0.028	0.031	0.042	460	546	521	525
56-4B	0.560	0.090	0.110	0.240	0.430	0.570	0.978	0.022	0.034	0.042	461	551	500	528
56-4C	0.570	0.090	0.110	0.240	0.518	0.482			0.034	0.037	560	647		509
56-8A	0.609	0.081	0.102	0.208	0.470	0.530	0.974	0.026			454	529	598	
56-11	0.620	0.070	0.090	0.220	0.555	0.445	0.984	0.016			501	582	492	
57-4D	0.530	0.068	0.086	0.316			0.984	0.016					466	
57-4E	0.473	0.039	0.034	0.454			0.988	0.012	0.034	0.041				524
57-4F									0.010	0.040				496
57-4H									0.017	0.041				508
57-4I									0.005	0.050				531
57-13A									0.020	0.045				526
Average (°C)											478§	546§	521	518
Std. dev. (°C)											29§	33§	43	12

Note: The $X_{i,ga}$ = mole fraction component i in garnet (al = almandine; py = pyrope; sp = spessartine; gr = grossular). $X_{i,bi}$ = i(Fe + Mg) in biotite; $X_{i,il}$ = i(Fe + Mg) in ilmenite; $X_{i,ca}$ = i/(Ca + Fe + Mg + Mn) in calcite.

* Garnet-biotite thermometry, calibration of Ferry and Spear (1978).

** Garnet-biotite thermometry, calibration of Hodges and Spear (1982).

† Garnet-ilmenite thermometry, calibration of Powneeby et al. (1987).

‡ Calcite-dolomite thermometry, calibration of Anovitz and Essene (1987, Equation 26).

§ Average temperature and standard deviation (1 σ) values exclude results for sample 56-4C.